

Spectroscopic properties of Y_3TaO_7 powders activated with Eu, Er and co-activated with Yb

Adam Walasek¹, Eugeniusz Zych^{1,*}, An Liqiong², Jian Zhang², and Shiwei Wang²

¹Faculty of Chemistry, University of Wrocław, 14 Joliot-Curie, 50-383 Wrocław, Poland

²Shanghai Institute of Ceramics, CAS, 1295 Dingxi Road, 200050 Shanghai, China

*corresponding author: zych@wchuwr.pl

Abstract. A new synthesis method of Y_3TaO_7 is reported. Pure phase powders were prepared by modified Pechini technique. Precursors obtained through that route were heated at the temperature about 1000°C with or without use of Li_2SO_4 flux. That implicates in different morphology of specimens and also their spectroscopic properties. Eu ions were used as a spectroscopic probe to prove inhomogeneous broadening of excitation and emission spectra. Samples with Er and Yb doping are also presented. Photoluminescence and up-conversion emissions, under 378 nm and 980 nm excitation respectively, strongly depend on the method of powders synthesis.

1. Introduction

Y_3TaO_7 crystallizes in a cubic structure with $a=5.25\text{\AA}$ [1, 2]. Interesting structural characteristic of that compound is that all metal ions ($3x\text{Y}$ and $1x\text{Ta}$) randomly occupy the same site offered by the host lattice. Also that system is O-deficient and location of O-vacancy varies from site to site [3]. Furthermore, from extended X-ray absorption fine structure (EXAFS) measurements it was found that a significant fraction of the triply ionized metal ions possesses more than one O-vacancy in their nearest surrounding [4]. These effects make Y_3TaO_7 a very interesting host lattice for spectroscopically active ions. We considered such structural characteristics favorable for up-conversion luminescence (UCL), where resonant or quasi resonant conditions between the involved levels of an activator and the excitation photons energy must be achieved to raise an electron to a high energy excited state [5] using lower-energy infrared photons. Similar approach was already described for CaGdAlO_4 and $\text{Ca}_3\text{Ga}_2\text{Ge}_4\text{O}_{14}$ doped with Er [6, 7].

UCL typically occurs through excited-state-absorption (ESA) process or energy-transfer (ET) mechanism [8]. In the former, two (or more) IR photons from the excitation beam are absorbed by the same ion of the activator in turn. In the latter the ion of activator absorbs one IR photon and the next portion of energy it gets from a neighboring ion which was also excited within the same time window or both portion of energy are transferred to the emitting center from two neighboring ions. Obviously, concentration of the various ions participating in the complex processes is very important and may determine which of the two possible mechanisms, ESA or ET, are more probable.

2. Synthesis and measurements

The synthesis was based on the known Pechini procedure. Tantalum chloride and yttrium nitrate (partially replaced by europium or erbium/ytterbium nitrate) were dissolved in ethanol and then citric

acid and ethylene glycol were added. That mixture was heated at temperature about 90°C until polymer was formed. Next the temperature was slowly increased to 600°C which led to carbonization and partial burning of organics. That raw powder was divided in two parts. One portion was directly heated in air at 1000°C for 5 hours and the other part was mixed with Li_2SO_4 flux and treated at the same conditions. Materials prepared using flux was recovered by washing with deionized water, filtering and drying in air at 200°C. The following notation will be used hereafter for the investigated materials. Samples made without flux: $\text{Y}_3\text{TaO}_7\text{:Er0.5\%}$ - sample E1, $\text{Y}_3\text{TaO}_7\text{:Er0.5\%,Yb5\%}$ - sample YE1. Samples prepared with the aid of flux: $\text{Y}_3\text{TaO}_7\text{:Er0.5\%}$ - sample E2, $\text{Y}_3\text{TaO}_7\text{:Er0.5\%,Yb5\%}$ - sample YE2. As spectroscopic probes of the activators environment in the host material we used Eu^{3+} ion. Hence for comparison we recorded excitation and luminescence spectra of $\text{Y}_2\text{O}_3\text{:Eu}$ (Philips Lighting) and $\text{Y}_3\text{TaO}_7\text{:Eu}$ (made using the flux aided route) powders to show the specific spectroscopic behavior of the activators in the Y_3TaO_7 host lattice. X-ray diffraction (XRD) patterns were measured with DRON diffractometer in the range of $2\theta=10\text{-}120$ degree with the step $\Delta\theta=0.1^\circ$ using $\text{Cu K}\alpha$ radiation ($\lambda=1.5418 \text{ \AA}$). Scanning electron microscopy (SEM) images were taken with JEM-2100F under an operating voltage of 200 kV. Photo excited luminescence (PL) spectra were recorded using F900 Spectrometer system (Edinburgh Instruments) equipped with a 450 W xenon lamp as excitation source and Hamamatsu R928P photomultiplier as the detector. For up-converted luminescence spectra measurements, an optical fiber coupled diode laser tuned to 980 nm was used as the excitation source, and the UCL spectra were recorded by the Fluorolog-3 spectrofluorometer. All emission spectra were corrected for the spectral response of the measuring system. The experiments were performed at room temperature.

3. Results and discussion

Fig. 1 presents representative XRD spectra for powders obtained with and without flux compared with theoretical pattern for Y_3TaO_7 . All spectra intensities are normalized to the same height. It is evident that the spectra obtained for our powders match perfectly the expected pattern for cubic Y_3TaO_7 . It is also clear that diffraction lines for powder obtained without flux are wider than for material obtained with the use of flux. This is suppose to come, according to the Scherrer's formula, from a nanocrystallinity of the materials prepared without the aid of flux [9]. Applying the Scherrer's analysis we get an average size of crystallites for all materials prepared without the use of flux (E1 and YE1, as well as the Eu-doped Y_3TaO_7 powder) about 14-15 nm. Powders prepared with the aid of Li_2SO_4 flux give narrow lines suggesting that the crystallites are larger than about 100 nm.

Fig. 2 shows SEM images for samples E1 and E2. They are fully representative for both class of powders (made without and with flux). The morphology of both powders is much different. For the sample E1 (as well as YE1 not presented here) we see large particles with sizes reaching 50-100 μm .

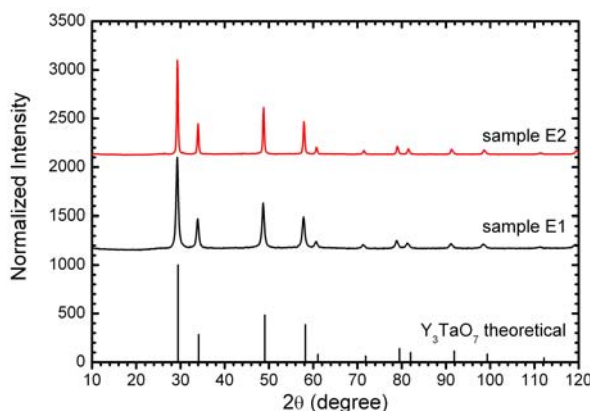


Figure 1. XRD patterns for Y_3TaO_7 powders heated in 1000°C with or without Li_2SO_4 flux compared with theoretical one.

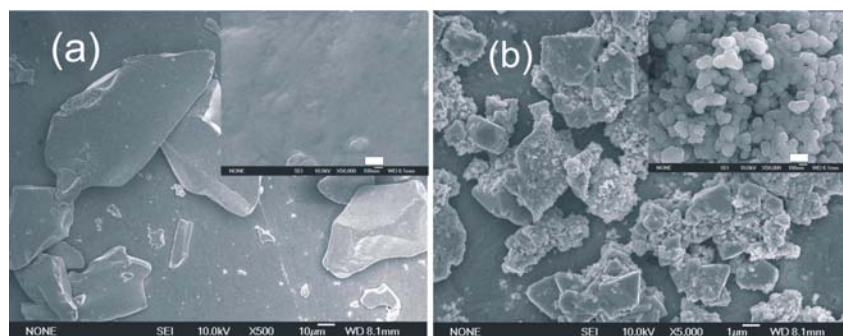


Figure 2. SEM images of sample heated without flux (a) and with addition of Li_2SO_4 (b). Insets show 50 000 times magnification of grains. Images are representative for both class of powders. The white bars in insets represent 200 nm.

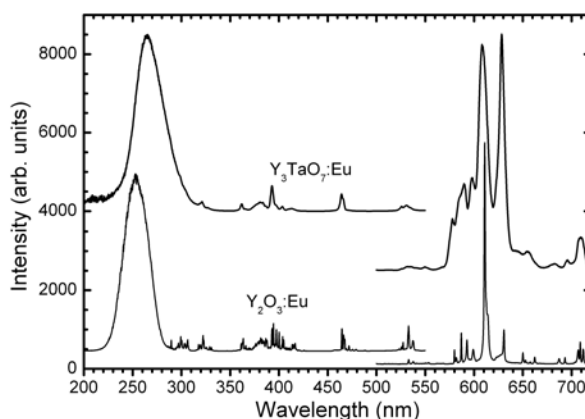


Figure 3. Eu^{3+} luminescence in Y_3TaO_7 compared with emission in Y_2O_3 host lattice. Note inhomogeneous broadening of f-f features in tantalate.

A high magnification of the grains, seen in the inset, does not show any additional structure. On the other hand, since the diffraction lines were significantly broadened, we suppose that the large grains are in fact agglomerates of nanocrystallites. Unfortunately, we could not make good quality TEM images since the particles were too thick to transmit electrons. Samples prepared with addition of flux, E2 and YE2, have different morphology. The particles are about 3-4 μm large and their surface is in most cases covered by a spherical structures, as exposed in the inset of Fig. 2b. We suppose that part of formed compound dissolves in the Li_2SO_4 flux and upon cooling it crystallizes on the surface of the earlier formed regular grains. This makes the powders made with flux somewhat non-uniform from the point of view of their morphology, unfortunately.

In Fig. 3 excitation (left) and emission spectra of $\text{Y}_2\text{O}_3:\text{Eu}$ and $\text{Y}_3\text{TaO}_7:\text{Eu}$ powders are presented. Although all spectra were recorded with the same resolution we can easily note that for Eu-doped yttria the lines are nicely separated and narrow as is expected for f→f transitions. The only exception is the broad band around 250 nm, which results from the $\text{O}^{2-} \rightarrow \text{Eu}^{3+}$ transition. For $\text{Y}_3\text{TaO}_7:\text{Eu}$ the f→f transitions are much broader and they have a band-type structure, not typical for lanthanides in crystalline environment. Results presented in Fig. 3 prove our supposition that the excitation/emission features in the Y_3TaO_7 should exhibit an inhomogeneous broadening due to the specific structure of the host lattice. The effect is rather significant, comparable to what is observed in glasses.

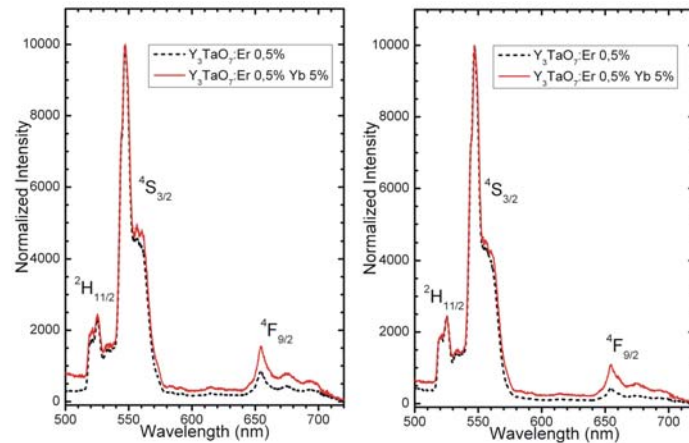


Figure 4. Photoluminescence spectra excited with 378 nm wavelength for both types of powders: heated without (left) and with addition of flux (right). Spectra are normalized at the 545 nm.

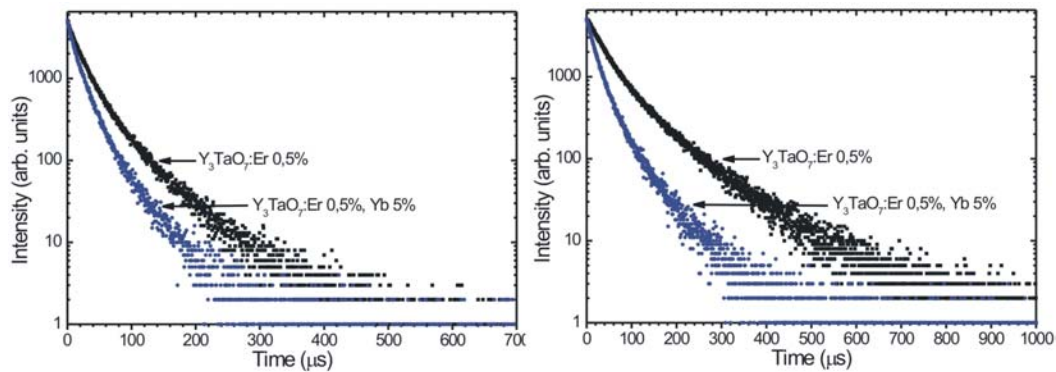


Figure 5. Decay traces of the 545 nm photoluminescence upon 378 nm excitation for powders heated without (left) and with addition of flux (right). Note the systematic shortening of the decay kinetics with Yb addition. See also Table 1.

Table 1. Average time constants of the 545 nm photoluminescence decays for the investigated materials.

Sample	Composition	Average time constant [μs]
E1	Y ₃ TaO ₇ :Er0.5%	30.6
YE1	Y ₃ TaO ₇ :Er0.5%, Yb5%	18.2
E2	Y ₃ TaO ₇ :Er0.5%	62.8
YE2	Y ₃ TaO ₇ :Er0.5%, Yb5%	28.5

Fig. 4. presents photoluminescence spectra of Y₃TaO₇ doped with Er or co-doped with Er and Yb for all E1, YE1 (left) and E2, YE2 samples. It is immediately seen that the photoluminescence spectra are very similar independently on the synthesis technique and of the composition. Only a small enhancement of the red component can be noted when Yb is present. Hence, basically two bands localized around 550 nm (green emission) and 660 nm (red emission) are observed. They can be ascribed to the $^2H_{11/2}/^4S_{3/2} \rightarrow ^4I_{15/2}$ and $^4F_{9/2} \rightarrow ^4I_{15/2}$ radiative transitions, respectively. Spectra are normalized at 545 nm wavelength to better reveal changes in intensity ratio between the components. Nevertheless, we can say that the most intense luminescence is observed for the material E2 – Er-doped Y₃TaO₇ prepared with the aid of Li₂SO₄ flux. The photoluminescence has green colour for all samples. As expected, all the emission features are much broader than typically observed for crystals[10, 11, 12]. The reason of such effect we discussed in introduction.

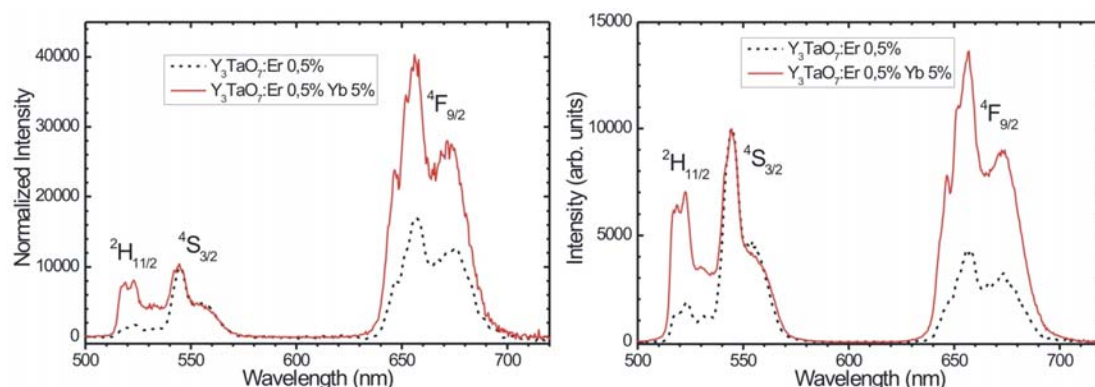


Figure 6. Up-converted spectra excited with 980 nm diode laser for powders heated without (left) and with addition of Li_2SO_4 (right). Spectra are normalized at the 545 nm.

It could be easily seen by eye that the photoluminescence intensity was lower for the co-doped samples YE1 and YE2 comparing to the Er-activated specimens E1 and E2, respectively. Measurements of decay traces of the most intense luminescence located around 545 nm, presented in Fig. 5, indeed showed that this emission is being partially quenched. Clearly, with Yb co-doping the decay time of the emission shortened noticeably. The time constants derived from the decays are given in Table 1 and prove this conclusion. At present we cannot yet offer a precise mechanism standing behind this quenching effect. Definitely, the Yb^{3+} levels have to be involved in this process. It may be that it is the $\text{O}^{2-}\text{-Yb}^{3+}$ charge transfer state, which is suppose to be located at rather low energies, which is responsible for the observed draining of energy from the emitting levels of Er^{3+} .

Fig. 6 shows up-conversion spectra of four specimens on which we report in this paper. We again normalized the spectra around 545 nm to better see the variations of emission color. While, similarly as in photoluminescence, again we get two luminescent bands located around 550 and 660 nm, their intensities ratio are now much different and significantly depends on the composition. Yb addition strongly enhances the relative intensity of the red component around 660 nm. The assignment of the UCL bands is given in Fig. 5. The total efficiency of the UCL is the highest for the specimen YE2 – co-doped with Er and Yb and fabricated with the aid of flux. Because the green component is always quite strong the UCL never appears purely red in color. In contrast to the photoluminescence the Yb addition exerts a profound influence on the spectral distribution of the UCL.

An interesting characteristics of the UCL emissions is that for the samples treated without flux (E1 and YE1) the red band is always relatively stronger comparing to the green one than it is seen for the samples processed with the Li_2SO_4 flux (E2 and YE2). This means that the probability of non-radiative dissipation of energy in the samples E1 and YE1 is higher than in E2 and YE2, respectively. If so, we could further assume that the nanocrystalline powders E1 and YE2 offers better conditions for non-radiative relaxation. Whether this occurs due to a higher population of defects – maybe traces of residuals after the preparation, or other imperfection in the structure, like strains - is not yet clear for us. However, the effect is systematic and has to have its source in the different method of synthesis. Note that from the XRD and SEM images we concluded that in the E1 and YE1 specimens the nanocrystallites agglomerates forming larger structures. Within the grain boundaries there must appear strain and some structural inaccuracy, which may partially contribute to the observed effect too.

Because the Yb^{3+} addition always improve effectiveness of UCL luminescence, it is obvious that this ion is involved into the process. From the position of levels of both Er^{3+} and Yb^{3+} [13] it is easy to find that excited Yb^{3+} can easily pass its energy to the nearby located Er^{3+} ion. Another IR excitation photon can also be delivered to already excited Er^{3+} by another Yb^{3+} excited within the same

time window. Since concentration of Yb is rather high the probability that two Yb^{3+} ions are located close enough to an Er^{3+} to cooperatively pass two quanta of excitation energy to the activator has to be also high, rather. We have to remember that absorption cross-section of Yb^{3+} for the 980 nm photons

is much higher than it is in the case of Er^{3+} [14]. Further, the concentration of Yb is at least by order of magnitude higher than Er. Therefore, it is Yb^{3+} which is expected to absorb the excitation photons rather in the co-doped systems. Hence, Er^{3+} gets this energy thanks to energy transfer from Yb^{3+} .

In the case of materials without Yb, Er^{3+} ions have no competition from other centers for the excitation energy. Hence the UCL in the E1 and E2 specimens has to occur through a sequential interception of two IR photons from the excitation beam by the same Er^{3+} ion. Possibility that two different Er^{3+} ions are excited and one of them passes its energy to the other one (possible considering *only* the position of energy levels [15, 16] of the activator) has to be excluded as the very low concentration of Er resulting in rather large distances between the ions of the activator must make the process inefficient.

4. Conclusions

Cubic phase of Y_3TaO_7 powders doped with Er or co-doped with Er and Yb were synthesized using modified Pechini technique and also using Li_2SO_4 flux. The flux influenced strongly the final powder morphology. A characteristic feature of all spectra was an inhomogeneous broadening of the $f \rightarrow f$ lines resulted from a structural disorder of the host lattice. Yb co-doping influenced the color of UCL making it much more reddish. Addition of ytterbium enhances significantly the total UCL intensity. However, this ion reduces the total efficiency of photoluminescence. In the co-doped materials energy from the excitation beam is being absorbed mostly by Yb^{3+} ions which pass the acquired excess of energy to the nearby located Er^{3+} . Hence the UCL in the co-doped samples has co-operative character.

Acknowledgements

Support from Minister of Science and High Education under grants No. N205 015 32/0721 and N205 024 31/1207 is acknowledged.

References

- [1] Allpress J G, and Rossell H J 1979 *J. Solid State Chem.* **27** 105-114
- [2] Wakeshima M, Nishimine H, and Hinatsu Y 2004 *J. Phys. Condens. Matter* **16** 4103-4120
- [3] Yokogawa Y, Yoshimura M, and Somiya S 1988 *Solid State Ionics* **28-30** 1250-1253
- [4] Tanaka T, Ishizawa N, Yoshimura M, Maruno F, and Oyanagi H 1995 *J. Solid State Chem.* **114** 79-87
- [5] Francini R, Pietrantonio S, Zambelli M, Speghini A, and Bettinelli M 2004 *J. Alloys Compd.* **380** 34-38
- [6] Yamaga M, Kodama N, Yosida T, Henderson B, and Kindo K 1997 *J. Phys.: Condens. Matter* **9** 9639-9649
- [7] Wells J-P R, Han T P J, Yamaga M, Kodama N, and Gallagher H G 2000 *J. Lumin.* **87-89** 1093-1095
- [8] Auzel F *Chem. Rev.* 2004 **104** 139-173
- [9] Klug H P, and Alexander L E 1974 *X-ray Diffraction Procedures For Polycrystalline and Amorphous Materials* (Second Edition) A Wiley-Interscience Publication John Wiley & Sons
- [10] Guo H, Li Y, Wang D, Zhang W, Yin M, Lou L, and Xia S 2004 *J. Alloys Compd.* **376** 23-27
- [11] Wang D, Yin M, Xia S, Makhov V N, Khaidukov N M, and Krupa J C 2004 *J. Alloys. Compd.* **368** 337-341
- [12] Mateos X, Solé R, Gavalda J, Aguiló M, Díaz F, and Massons J 2005 *J. Lumin.* **115** 131-137
- [13] Liu M, Wang S W, Zhang J, An L Q, and Chen L D 2007 *Opt. Mater.* **29** 1352-1357
- [14] de Camargo A S S, Nunes L A O, Silva J F, Costa A C F M, Barros B S, Silva J E C, de Sá G F, and Alves Jr S 2007 *J. Phys.: Condens. Matter* **19** 246209 (7pp)
- [15] Philipps J F, Töpfer T, Ebendorf-Heidepriem H, Ehrh D, and Sauerbrey R 2002 *Appl. Phys. B* **74** 233-236
- [16] Georgescu S, Toma O, Florea C, and Naud C 2003 *J. Lumin.* **101** 87-99